Biochimica et Biophysica Acta, 1066 (1991) 115–123

ADONIS 000527369100267R

BBAMEM 75265

Changes in cellular membrane and paracellular conductances by amphotericin B in the epithelium of the bullfrog cornea

Peter S. Reinach [1,*], John T. Tarvin [2] and Michel Hirsch [3]

[1] *Department of Ophthalmology, Washington University School of Medicine, St. Louis, MO (U.S.A.),* [2] *Department of Physics and Astronomy, Murray State University, Murray, KY (U.S.A.) and* [3] *Centre National de la Recherche Scientifique, Laboratoire de Microscopie Electronique Appliquee a la Biologie, Paris (France)*

(Received 30 July 1990)
(Revised manuscript received 18 March 1991)

Key words: Cornea; Epithelium; Amphotericin B; Conductance; Capacitance; Impedance analysis; Cell coupling

In the isolated bullfrog cornea, measurements of DC electrical parameters in conjunction with AC impedance and ultrastructural analyses were used to determine the effects of 10^{-5} M amphotericin B on epithelial cellular membrane and paracellular conductances. In NaCl Ringers, amphotericin B elicited a 3.5-fold increase in the specific apical membrane conductance (G_a/C_a); where G_a and C_a are the apical membrane conductance and capacitance, respectively. The basolateral membrane conductance (G_b) and the basolateral membrane capacitance (C_b) fell by 57% and 50%, respectively. In the paracellular pathway, the tight junctional complex (G_j) was unchanged whereas the lateral intercellular space resistance (R_p) decreased by 55%. The declines in G_b and C_b were suggestive of cell volume shrinkage because these changes were consistent with a previously described decline in intracellular K^+ content and reduction in exposed basolateral membrane area to current flow. Ultrastructural analysis validated that amphotericin B caused cell volume shrinkage because there was: (1) increased folding of the basolateral membrane and waviness of the basal aspects- of the plasma membrane; (2) dilatation of the lateral intercellular spaces. This agreement suggests that intracellular activity decreased following exposure to amphotericin B which resulted in cell volume shrinkage and an impairment of Cl^- uptake across the basolateral membrane.

Introduction

In the isolated bullfrog cornea, more than 90% of the short-circuit current (I_{sc}) is accounted for by active transepithelial Cl^- transport from the stromal to the tear-side bathing solution [1]. Net translocation is a consequence of uptake through a basolateral membrane Na/Cl symport followed by electrodiffusion across the apical membrane into the tears. The driving force for Cl^- uptake is the downhill cell directed Na^+ gradient maintained by the activity of the Na^+/K^+ pump in the basolateral membrane [2]. Electrodiffusion across the apical membrane is partially dependent on K^+ recycling between the stromal-side bathing solution and the cell interior [3].

The mechanism of net ion translocation across the basolateral membrane was studied following exposure to either amphotericin B or nystatin. These quasi-ionophores increased cation apical membrane cation permeability, which altered intracellular ion composition, and thereby elicited increases in Na^+/K^+ pump activity as well as rates of net Na^+ and K^+ transport [4–13]. However, unexplainedly net Cl^- transport decreased [7]. The mechanism accounting for this decline was not further considered because the use of DC circuit analysis required too many simplifying assumptions whose validity may be open to question [4,5]. Accordingly, there are no studies available in which DC circuit analysis was used to analyze the effects of amphotericin B on net ion transport in NaCl Ringers. Another approach is to use AC impedance analysis which has the attribute of not requiring any assumptions regarding the selectivity of a modulatory agent in only modifying a single element in the electrical equivalent [14].

We used the measurements of DC electrical param-

* Correspondence (present address): P.S. Reinach, Department of Physiology and Endocrinology, Medical College of Georgia, Augusta, GA 30912, U.S.A.

eters in conjunction with AC impedance and ultrastructural analyses to determine how exposure to amphotericin B caused a decline in Cl^- secretion. The results indicate that a decrease in intracellular ionic activity elicited cell volume shrinkage and impaired net Cl^- uptake across the basolateral membrane as well as Cl^- efflux across the apical membrane into the tears.

Materials and Methods

The corneas of double pithed bullfrogs (*Rana catesbeiana*) were excised and vertically mounted, with silicone vacuum grease, in a modified Ussing chamber using a previously described method [15]. In most cases, the cornea was supported by a hemispherical piece of nylon mesh. The tear-side of the chamber was open on top to allow access of a microelectrode. Ag-AgCl electrodes, prepared by dipping silver wire into molten silver chloride, were used for current sending and for voltage measurement [14]. The voltage sensing electrodes were positioned as close to the tissue as possible in order to minimize series solution resistance. Each half-chamber had a volume of 3 ml; the nominal tissue area was 0.5 cm^2.

At room temperature, the isolated cornea was bathed symmetrically with a room air equilibrated Ringer's solution. The solution had the following composition (in mM): NaCl 111.0, KOH 2.5, $CaCl_2$ 1.0, $MgCl_2$ 1.0, and Hepes 1.0 (pH 8.1). The corneas were exposed to 10 μM amphotericin B on the tear-side. This concentration was obtained by adding the drug with a micropipette to the tear-side from a 1000-fold more concentrated stock solution (Squibb).

Transepithelial voltage, transepithelial conductance (g_t) and/or short-circuit current (I_{sc}) were measured as previously described using a voltage/current clamp amplifier (Biomedizinische Gerate, Germering, Munich, F.R.G.) [3,6,9,16]. The outputs were monitored on a 6-channel chart recorder (model Servogor 460, BBC-Metrawatt/Goerz, Broomfield, CO). Conventional microelectrodes were pulled on a horizontal puller (model PD-2, Narishige, Japan) from 1.2 mm borosilicate glass (Hilgenberg Glas, Malsfeld, F.R.G.) and backfilled with filtered 3 M KCl (15 to 50 Mohm). Membrane voltage, V_{sc}, under short-circuit current conditions, and the relative apical membrane resistance ratio, fR_0 were obtained with a microelectrode amplifier (Biomedizinische Gerate, Germering, Munich, F.R.G.) using a previously described protocol [3,6,9,16]. The tissue was intermittently short-circuited during brief periods to measure the I_{sc} and the g_t; otherwise it was left open-circuited for measurements of the a.c. electrical parameters.

Calibration values for fR_0 were obtained in a separate set of corneas (cf. Fig. 1). These values were determined over the same time intervals during which

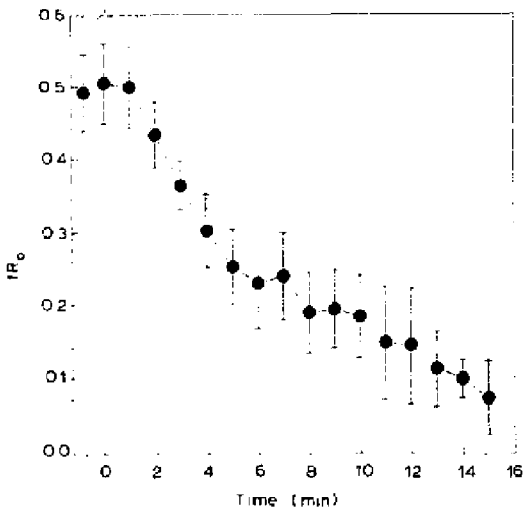

Fig. 1. Decreases in fractional apical membrane resistance, fR_0, in NaCl Ringers following exposure to 10^{-5} M amphotericin B. To perform AC impedance analysis, these values were determined in a separate set of corneas under the same conditions as those used to measure the a.c. electrical parameters.

the a.c. electrical parameters were measured. Validation criteria for an adequate impalement required that : (1) the membrane voltage was stable ($\pm$2 mV), (2) fR_0 was stable ($\pm$2%) for at least 3 min and (3) the microelectrode's resistance remained stable at a value that was less than 10 Mohm larger than its solution value.

Transepithelial impedance was measured over the range (after correction for aliased points) of 0.2 Hz to about 8 KHz in three overlapping domains of three decades using for each a pseudo-random binary current (10 $\mu A/cm^2$ peak-to-peak) technique [14]. Briefly, the voltage response of the tissue to the above current was amplified (model 113, Princeton Applied Research, Princeton, NJ), anti-alias filtered (Wavetek San Diego, Inc., San Diego, CA), and digitized (model DT2801-A, Data Translation, Inc., Marlboro, ME). The entire sequence of signal generation, data collection and storage was under the control of an 8 MHz Deskpro Model 4 personal computer (Compaq Computer Corp., Houston, TX) equipped with an 8087 coprocessor. In order to improve the signal-to-noise ratio, the data was signal averaged in the time domain prior to transforming it (via a fast Fourier transform) to the frequency domain. Collection of a single, three-decade set of data generally took less than 2 min with our protocol for signal averages (i.e. 4–100 scans) in the indicated frequency ranges (i.e. 0.2–80, 2–800, 20–8,000 Hz). From these measurements, 96–100 points approximately equally spaced on a log scale, were chosen as input for the non-linear least-squares curve-fitting program. During a cornea's control pe-

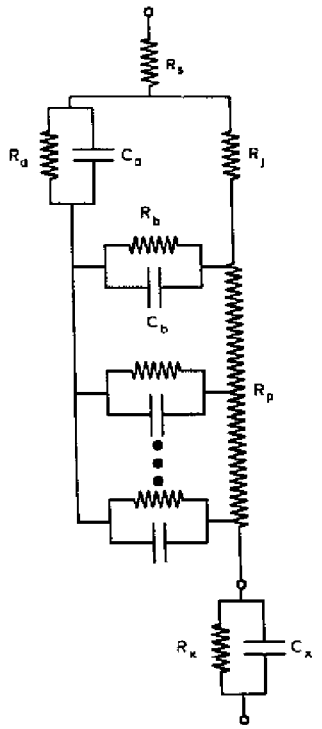

Fig. 2. Distributed equivalent-circuit model for the corneal epithelium. Conductances: G_a, G_b and G_j are apical, basolateral membranes and tight junctional complex, respectively. Resistances: R_p and R_s are lateral intercellular space and solution, respectively. Capacitances: C_a and C_b are apical and basolateral membranes, respectively. The equivalent for the endothelium is represented by R_x and C_x.

riod, following stabilization of the I_{sc}, the tissue's impedance was measured at three different times and the means were obtained of the calculated values of the fitted parameters.

The impedance data were fit to the previously described morphologically derived equivalent-circuit model shown in Fig. 2 using a derivative-free Levenberg-Marquardt algorithm [14]. The *R*-factor was used as a measure of the quality of the fit. The average value of the *R*-factor obtained in most fits was less than 1% but never exceeded 2%. All computations were performed on the Compaq personal computer. The details of this technique have been previously described [14]. All statistical tests were performed using Sigmaplot 4.0 (Jandel Scientific Corte Madera, CA) and are based on a paired Student's *t*-test.

Corneas were dissected and placed in NaCl Ringers and incubated for 14 min with 10^{-5} M amphotericin B (i.e. the time shown in Table I that was required to elicit maximal stimulation of the I_{sc}). The whole corneas were fixed in 2. 5% glutaraldehyde in 0.1 M phosphate buffer (pH 7.4) at room temperature. After 1 h, the central part of the corneas was cut into small pieces and immersed in the same fresh fixative for an additional 2 h. After rinsing, the samples were post-fixed in 1% buffered osmium tetroxide for 1 h, dehydrated in alcohol and embedded in Epon 812. Ultrathin uranyl acetate and lead citrate contrasted sections were then observed in a Philips EM 300 electron microscope. All micrographs were photographed with a magnification of 4400× and then enlarged to 6600×. Computer aided morphometry was performed to determine surface area of *n* cells for profiles showing a defined midsection of nucleus and a specific corneal epithelial thickness.

Freeze-fracture studies were performed on glutaraldehyde-fixed samples. They were cryoprotected in 25% glycerol in buffer for 2 h, mounted between two copper discs and rapidly frozen in solid-liquid nitrogen. Platinum-carbon replicas of non-etched fractured specimens were produced in a cryofract CF 250 freeze-fracture apparatus (Reichert-Jung Cambridge Instruments) equipped with electron beam guns and a quartz thickness film monitor at a stage temperature of −150°C and a vacuum of at least 10^{-7} torr. Cleaned replicas were then observed in a Philips EM 300 electron microscope.

Results

To identify any changes in epithelial morphology that accompany a 14 min exposure to amphotericin B, electron micrographs and freeze-fracture replicas were obtained. The micrograph of a control shown in Fig. 3A indicates that it is not possible to identify any intercellular separations. Although the control micrograph shows areas of direct contact through desmosomes, there are no recognizable intercellular spaces: the neighboring cells make close tortuous contacts with one another making it impossible to estimate the dimensions of the intercellular spaces.

In the amphotericin B-treated cornea (cf. Fig. 3B), there are distinct changes in the cellular morphology and the widths of the lateral intercellular spaces. The basolateral membranes are wavy and convoluted and the lateral intercellular spaces are clearly evident. The separation is so pronounced that the desmosomes have disappeared. Computer aided morphometry indicated a 26% decrease in exposed membrane surface area from the controls. All of these changes are consistent with cell shrinkage. The dilatation elicited by amphotericin B is further documented by the change shown in the freeze fracture replicas provided in Fig. 4.

The individual control and stimulated values of the I_{sc} and the g_t after a 14 min exposure are provided in Table I. The I_{sc} and g_t increased by 100% and 25%, respectively. As previously described, at later times there were secondary changes in g_t resulting from a decrease in paracellular resistance [5]. Accompanying

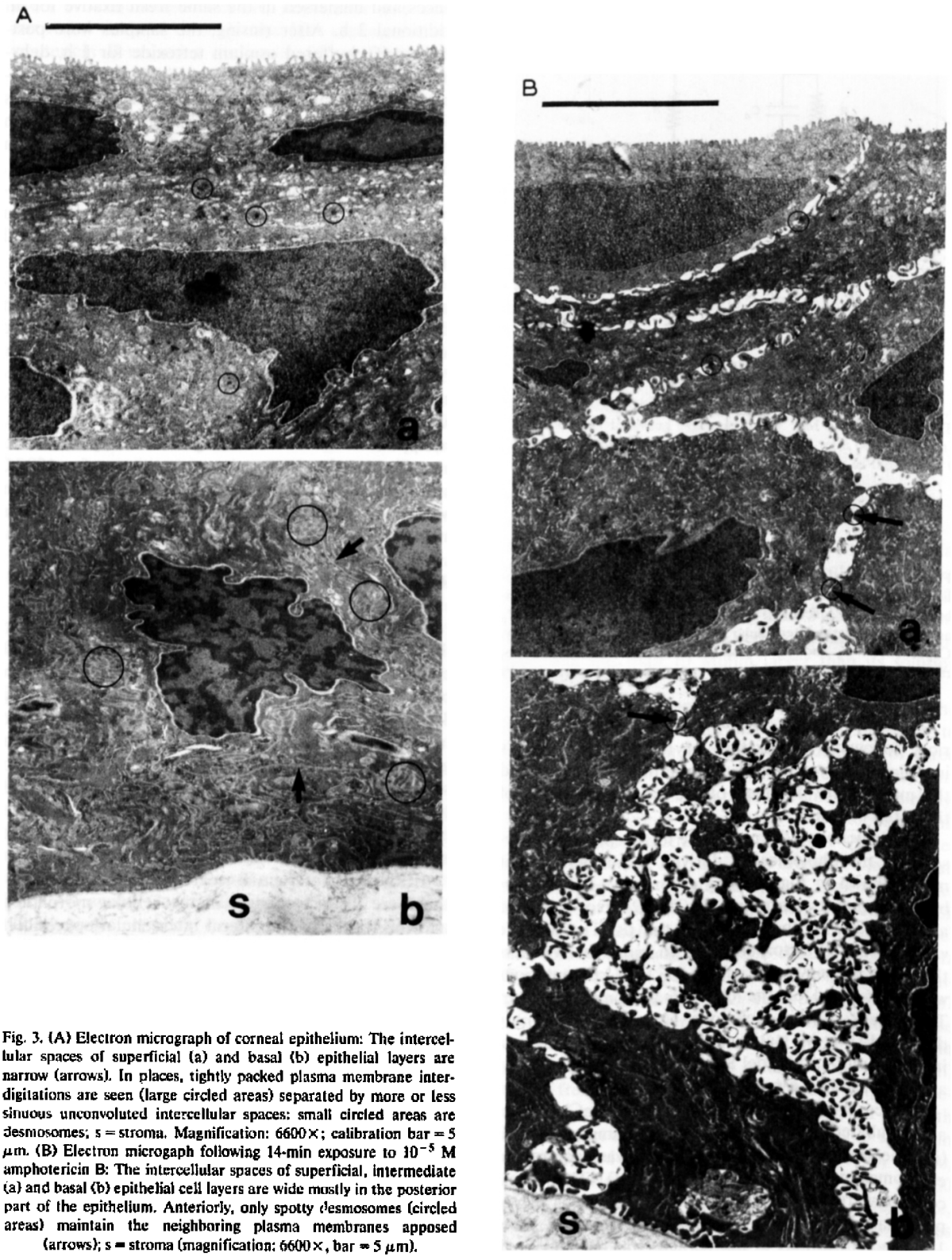

Fig. 3. (A) Electron micrograph of corneal epithelium: The intercellular spaces of superficial (a) and basal (b) epithelial layers are narrow (arrows). In places, tightly packed plasma membrane interdigitations are seen (large circled areas) separated by more or less sinuous unconvoluted intercellular spaces: small circled areas are desmosomes; s = stroma. Magnification: 6600×; calibration bar = 5 μm. (B) Electron micrograph following 14-min exposure to 10^{-5} M amphotericin B: The intercellular spaces of superficial, intermediate (a) and basal (b) epithelial cell layers are wide mostly in the posterior part of the epithelium. Anteriorly, only spotty desmosomes (circled areas) maintain the neighboring plasma membranes apposed (arrows); s = stroma (magnification: 6600×, bar = 5 μm).

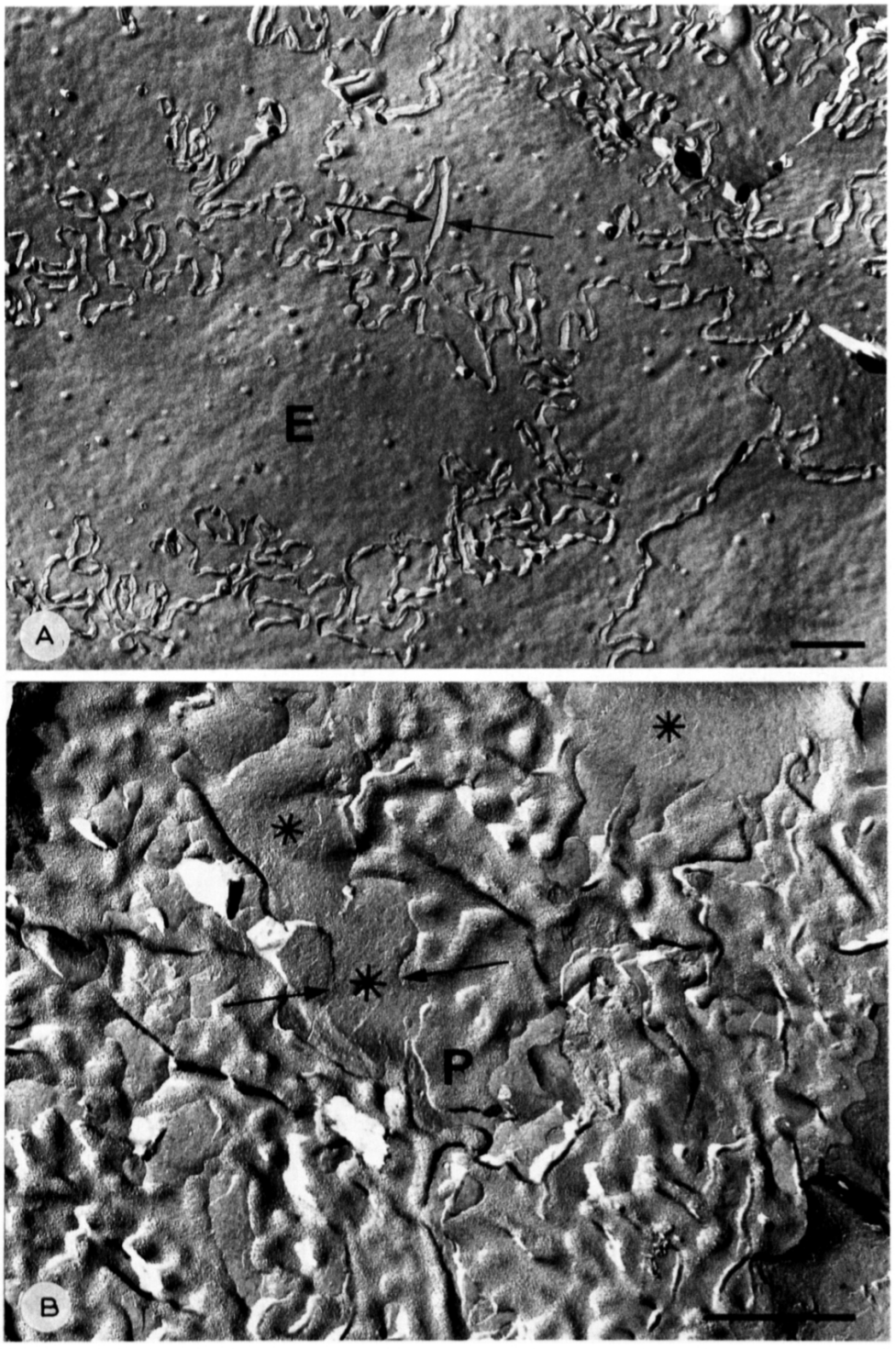

Fig. 4. (A) Freeze-fracture electron micrograph of corneal epithelium: exoplasmic leaflet (E) of basal plasma membranes of basal epithelial cells separated with narrow sinuous intercellular spaces (between arrows) (12500×; bar = 1 μm). (B) Freeze-fracture electron micrograph following amphotericin B exposure: protoplasmic leaflet (P) of basal plasma membranes of basal epithelial cells separated with very large intercellular spaces in places (asterisks and between arrows) (magnification: 24000×; bar = 1 μm).

TABLE I

Effect of 10 μM amphotericin-B on d.c. parameters

Run	State	I_{sc} ($\mu A/cm^2$)	G_t (mS/cm^2)	fR_0
1.1	Control	−16.7	2.04	0.38
1.2	Ampho	−20.6	2.48	0.07
2.1	Control	−12.3	1.44	0.48
2.2	Ampho	−25.8	2.00	0.09
3.1	Control	−3.5	1.85	0.53
3.2	Ampho	−7.5	1.72	0.04
4.1	Control	−12.0	0.73	0.67
4.2	Ampho	−27.2	0.89	0.15
5.1	Control	−9.4	0.57	0.33
5.2	Ampho	−20.0	0.79	0.03
6.1	Control	−8.5	1.00	0.69
6.2	Ampho	−23.8	1.16	0.17
7.1	Control	−10.8	0.99	0.78
7.2	Ampho	−16.2	1.14	0.17
	Control	−10	1.2	0.55
	S.E.	2	0.2	0.06
	Ampho	−20	1.5	0.10
	S.E.	3	0.2	0.02
	P(paired)	< 0.05	< 0.05	< 0.05

increases in the I_{sc}, the specific apical membrane conductance (G_a/C_a) increased 3.5-fold from its control value (cf. Fig. 5). The time course of these increases paralleled those of the I_{sc} which is consistent with the notion that the apical membrane is the rate limiting barrier for net ion transport [4,5,7,14]. The apical

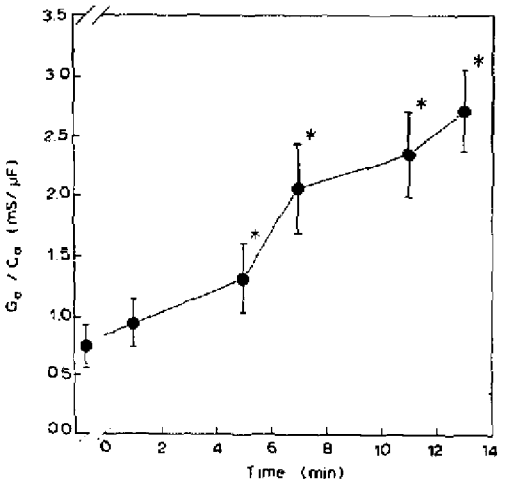

Fig. 5. Time-dependent effects of 10^{-5} M amphotericin B on apical membrane conductance ($n = 7$). G_a was normalized to C_a to obtain specific apical membrane conductance. The control value prior to amphotericin B is shown to the left of the break in the abscissa. Values are shown as means±S.E. Significance ($P < 0.05$) determined with paired *t*-test. Asterisk indicated value is significantly different with respect to control. All the values were significantly different from the control except for the 0–2-min period.

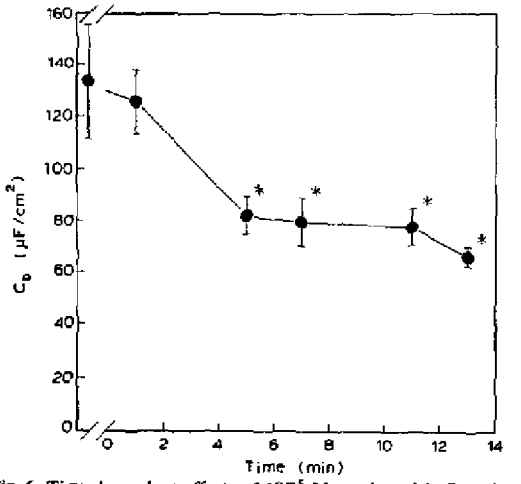

Fig. 6. Time-dependent effects of 10^{-5} M amphotericin B on basolateral membrane capacitance ($n = 7$). See legend to Fig. 5 for details. All of the changes were significantly different from the control period except for the 0–2-min period.

membrane capacitance, C_a, is reflective of apical membrane area through the well-known relationship (1 cm^2 = 1 μF) [14,17]. Therefore, extraction of membrane capacitance in the fitting procedure and normalizing it to the membrane conductance allows estimation of the specific membrane conductance. In this study, the control value of C_a was 2.0 ± 0.1 $\mu F/cm^2$ ($n = 7$) compared to a value of 2.6 ± 0.6 $\mu F/cm^2$ in the 12–14-min period following exposure to amphotericin B. This change was not significant ($P > 0.05$, paired *t*-test) suggesting that amphotericin B had no effect on apical membrane area.

The time-dependent effects of amphotericin B on the basolateral membrane capacitance C_b are shown in Fig. 6. The much larger value for the basolateral membrane capacitance, C_b, is consistent with that previously reported and was attributed to cell to cell coupling between and across the cell layers of the epithelium [14]. This coupling effect means that the effective basolateral membrane area actually constitutes all the membrane area in the deeper layers rather than just the basolateral membrane area within a single cell or layer. It is apparent that C_b decreased continuously and that in the 4–6-min period the decline became significant with respect to the control value. In the 12–14-min period the value for C_b was (66 ± 38 $\mu F/cm^2$) only 50% of the control value (i.e. 133 ± 22 $\mu F/cm^2$). This decrease, in conjunction with the changes seen in the electron micrographs and freeze fracture replicas (cf. Figs. 3 and 4), suggests that the decrease in C_b may reflect cell volume shrinkage which in turn leads to electrical uncoupling between cells in the same and other layers.

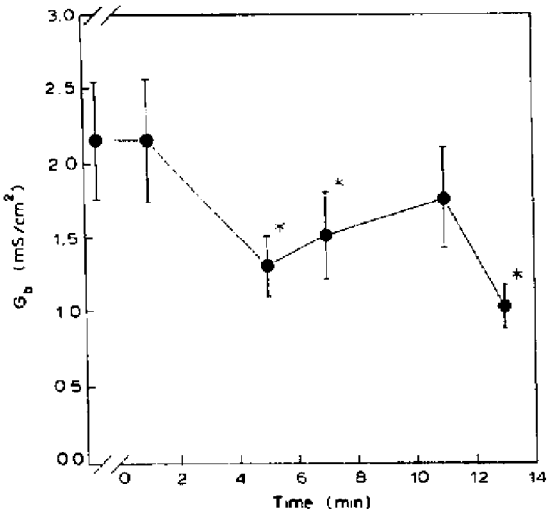

Fig. 7. Time-dependent effects of 10^{-5} M amphotericin B on basolateral membrane conductance. See legend to Fig. 5 for details. All of the changes were significantly different from the control period except for the 0–2- and 10–12-min intervals.

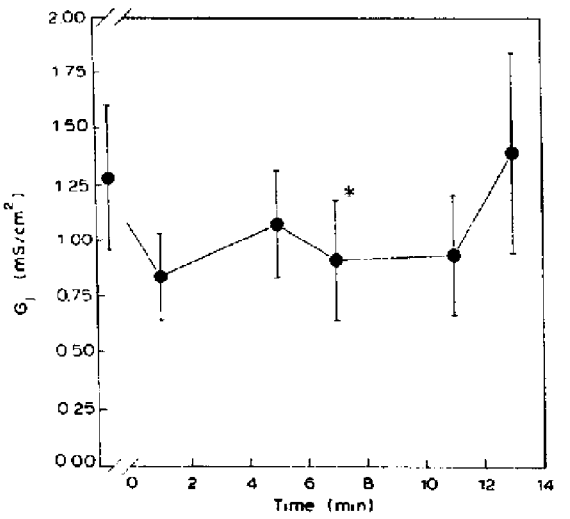

Fig. 8. Time-dependent effects of 10^{-5} M amphotericin B on tight junctional complex conductance. See legend to Fig. 5 for details. Note there were no significant changes except at the 6–8-min interval.

The effects on G_b shown in Fig. 7 indicate that in the first two min period, G_b was unaffected by amphotericin B. However, at all the later time periods G_b was significantly less than the control value of 2.2 ± 0.4 mS/cm^2. The first significant decrease occurred in the 4–6-min period. Neither of the calculated values in the 6–8- and 10–12-min periods were significantly different from the value in the 4–6-min period. Note that G_b declined further in the 12–14 min to a value that was 43% of its control.

The correspondence was considered between the changes in the ultrastructure and the equivalents of the paracellular pathways: G_j and R_p. Except for the 6–8-min period, none of the changes in G_j were significant with respect to the control period (cf. Fig. 8). This lack of a consistent effect on G_j, which is the rate-limiting barrier in the paracellular pathway, is in general agreement with very subtle acute changes in the shunt conductance in Cl-free Ringers [4,5]. However, the time-dependent effects on R_p shown in Fig. 9 indicate that it uniformly and continuously declined. In the 12–14-min interval, R_p was only 55% of the control value (i.e. 254 ± 28 to 139 ± 15 ohm cm^2). Except for the initial 2–4-min period, all the later values for R_p were significantly different from its control period value. These decreases in R_p are consistent with the widening of the lateral intercellular spaces observed in the micrographs and with the decreases in G_b and C_b. This dilatation effect is suggestive of cell volume shrinkage which causes infolding of exposed membrane and thus reduces membrane accessibility to current flow.

As shown previously, the quality of the fits of the measured to the predicted impedances were significantly improved with the inclusion of series elements that are thought to be representative, in terms of the model shown in Fig. 2, of: (1) the solution resistance, R_s; (2) the endothelium, R_x and C_x [14]. Under control conditions, R_s was 76 ± 5 ohm cm^2. It declined to 70 ± 5 ohm cm^2 in the 12–14-min period following the addition of amphotericin B. Even though amphotericin B decreased R_s by only 6 ohm cm^2 (i.e. 8%), this decline was consistent in all experiments and was

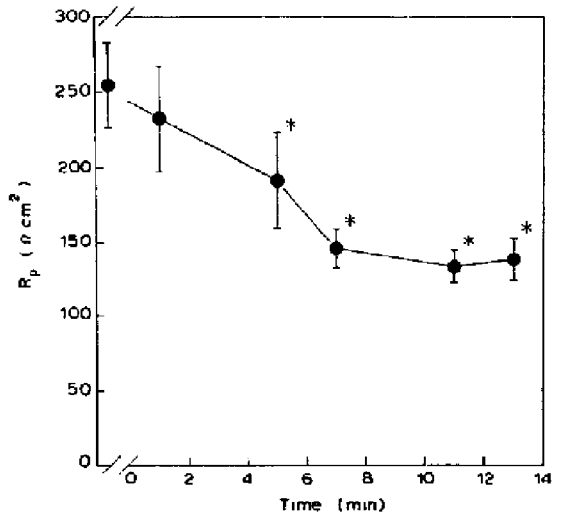

Fig. 9. Time-dependent effects of 10^{-5} M amphotericin B on lateral intercellular space resistance. See legend to Fig. 5 for details. All of the changes were significant except the 0–2-min interval.

therefore significant ($P < 0.05$) using a paired t-test. With regards to R_x, amphotericin B significantly decreased R_x from 27 ± 2 ohm cm^2 to 18 ± 2 ohm cm^2 in the 12–14-min period. Amphotericin B had no significant effect on C_x which varied somewhat randomly between 3.9 ± 0.6 and 3.2 ± 0.9 μF/cm^2.

Discussion

We used measurements of d.c. electrical parameters, in conjunction with alternating current (a.c.) impedance and ultrastructural analyses, to identify the mechanism of a reduction in active Cl^- transport following exposure to amphotericin B. The values extracted from the distributed model to analyze the impedance response are consistent with those previously obtained using d.c. circuit analysis in Cl-free Ringers [4,5,7]. However, with our approach, it was possible for the first time to resolve changes in specific cellular membrane conductance from those in the paracellular pathway and thereby determine the effects of amphotericin B on apparent cell volume. In reversing the direction of net ion transport from secretion to absorption, amphotericin B caused shrinkage which suggests that the lateral intercellular spaces may provide the osmotic compartment for fluid accumulation.

There was a 3.5-fold increase in the specific apical membrane conductance (G_a/C_a). This change elicited apparent intracellular increases in Na^+ activity and a measured reciprocal decline in K^+ because the apical membrane permeability is rate limiting for Na^+ absorption towards the stroma and K^+ secretion into the tears [5,7]. The magnitude of the increase in Na^+ activity is unknown because there are no measurements of the effect of amphotericin B on intracellular Na^+ activity. Even though this change is not known, Na^+ must have increased to a level that was lower than the activity of the bathing solution (i.e. 86 mM) because Na^+ absorption persisted. Therefore, the Na^+ increase was less than 72 mM because this is the value for the difference between its control level (i.e. 14 mM) and that of the bathing solution. On the other hand, the magnitude of the decrease in intracellular K^+ activity is known because it decreased by 94 mM from 106 to 12 mM [2,5,6]. Therefore, the total loss of cationic activity was at least 22 mM. Since the basolateral membrane has an appreciable K^+ permselectivity, the large decline in intracellular K^+ activity explains why G_b declined [3–6].

A meaningful interpretation of the change in basolateral membrane capacitance (C_b) is only possible after a consideration of the effects of amphotericin B on ultrastructure. In the control, the basal aspect of the basal cell layer exhibits very sinuous intercellular clefts which are rather regular in width and the basal plasma membranes are flat. After amphotericin B treatment, large intercellular clefts appear and the basal plasma membranes are wavy. These changes coupled with increased basolateral membrane folding and the dilatation of the lateral intercellular spaces cast some doubt on the relevance of normalizing the basolateral membrane conductance to its capacitance so as to calculate a value for the specific basolateral membrane conductance (G_b/C_b). Were this done, it would overestimate a decline in basolateral membrane permeability because C_b is reflective of effective basolateral membrane area provided the cells had remained electrically coupled through gap junctions. Therefore, the effect of amphotericin B was not considered on specific basolateral membrane conductance.

Amphotericin B also had time dependent effects on the paracellular electrical equivalents and morphology that are consistent with one another. As was previously shown, the value for the tight junction conductance (G_j) is 4-fold less than R_p and therefore G_j is rate-limiting for ion permeation through this pathway. G_j did not change and this lack of an effect on G_j is for the most part consistent with previously measured small increases in Na^+ flux from stroma to tear and mannitol flux from tear to stroma [4,5]. However, R_p ultimately decreased by 55% which is consistent with the changes in the micrographs and freeze fracture replicas. The correspondence between the decrease in R_p and the dilatation of the spaces on the basal and lateral aspects of cells strengthens the notion that amphotericin B elicited a shrinkage in cell volume.

The results of both electrical and ultrastructural analyses point to an amphotericin B induced decrease in cell volume. This change stems from a fall in total intracellular ion activity. As indicated, this loss is caused by a measured loss in K^+ which exceeds an anticipated gain in Na^+. The identity of the accompanying anion(s) for the maintenance of electroneutrality is problematic. The membrane voltage depolarized to -15 mV and if the intracellular Cl^- activity were to rise to its predicted electrochemical equilibrium value it would have risen from 22 to 47 mM. However, such a change did not occur because Cl^- secretion is only partially suppressed by amphotericin B. In any case, Cl^- may not be the only counterion because the anticipated cation decrease is at least 22 mM which is equal to the intracellular Cl^- activity under control conditions.

The relationship between changes in apparent epithelial cell volume and stimulation of net ion transport is different in absorptive and secretory epithelia . In absorptive epithelia, stimulation of absorption by exposure to either amphotericin B or through an increase in Na^+ driven solute uptake is associated with dilatation of the intercellular spaces [18–20]. In contrast, with a secretory tissue, the corneal epithelium, the spaces appeared more constricted and collapsed following a selective stimulation of Cl^- secretion [21]. In this study,

the increase in dilatation of the lateral intercellular spaces and the decrease in R_p are both consistent with previous studies showing that amphotericin B caused a reversal in the direction of net ion transport from secretion to absorption [7]. This reversal reflected a large increase in net Na^+ absorption and induction of K^+ secretion to a level that was smaller than that of Na^+ absorption [5]. This change decreased the driving force established by the Na^+ chemical gradient for coupled Cl^- uptake across the basolateral membrane through the Na:Cl symport as well as the negativity of the electrical driving force for Cl^- efflux from the cells into the tears. All of these effects decreased Cl^- secretion and led to an increase in osmolality of the intercellular spaces which caused them to dilate.

Amphotericin B significantly decreased R_s by 8%. Clausen et al. attributed R_s to the finite resistance arising from the unstirred layers between the voltage-measuring electrodes and the apical and basolateral membrane surfaces [14]. If this assignment were correct, it is difficult to accept that amphotericin B could selectively decrease the resistance of the unstirred layers. In order for amphotericin B to decrease R_s by 6 ohm cm^2, the % decrease in the unstirred layer resistance would need to be much larger than 8% because its width is only about 10% of the separation between the two voltage sensing electrodes. Clausen et al. also had reservations regarding assignment of a precise correlate for R_s, in a study with stomach, because R_s appeared to be artifactually large [22]. Their interpretation was that, "the tissue must restrict diffusion more than does an equivalent thickness of free solution." Presumably, the small but significant decrease in R_s is associated with the "nonsolution" aspect of R_s. It should be noted that the significant change in R_s is associated with the direction of its change (i.e. a decrease) rather than the magnitude of its change since an independent t-test shows no signifcant change in R_s from its control value.

As previously found, the quality of fits of the data to the distributed model were significantly improved with the inclusion of elements represented by R_x and C_x [14]. Their physiological correlates were tentatively assigned to represent the parallel combination for endothelial membranes. The decreases in R_x only became significant in the 12–14-min period following exposure to amphotericin B. Such an effect could mean a slow increase in endothelial conductance, however, the physiological relevance of this finding is not yet apparent.

Acknowledgement

This work was supported by National Institutes of Health Grant, EY04795 to P. Reinach and MSU CISR Grants 2-12925, 2-12478 and NSF Grant RII-86-10671 to J. Tarvin. We are deeply endebted to Chris Clausen for his help in implementing the technique and helpful discussions during the preliminary phases of this work. The technical support provided by Gerald Gusdorf and Rachel Locke is deeply appreciated.

References

1 Zadunaisky, J.A. (1966) Am. J. Physiol. 211, 506–512.
2 Reuss, L., Reinach, P., Weinman, S.A. and Grady, T.P. (1983) Am. J. Physiol 244, C336–347.
3 Reinach, P. and Nagel, W. (1985) J. Membr. Biol. 87, 201–209.
4 Candia, O.A. and Cook, P.J. (1986) Am. J. Physiol. 250, F850–859.
5 Candia, O.A., Reinach, P.S. and Alvarez, L. (1984) Am. J. Physiol. 247, C454–461.
6 Reinach, P., Thurman, C. and Klemperer, G. (1987) J. Membr. Biol. 99, 205–213.
7 Candia, O.A., Bentley, P.J. and Cook, P.I. (1974) Am. J. Physiol. 247, C454–461.
8 Wolosin, M. and Candia, O.A. (1987) Am. J. Physiol. 253, C555–560.
9 Huff, J.W. and Reinach, P.S. (1985) J. Membr. Biol. 85, 215–224.
10 Reinach, P. and Schoen, H.F. (1990) Biochim. Biophys. Acta 1026, 13–20.
11 Carrasquer, G., Nagel, W., Rehm, W. and Schwartz, M. (1987) Biochim. Biophys. Acta 990, 258–266.
12 Carrasquer, G., Rehm, W. and Schwartz, M. (1986) Biochim. Biophys. Acta 862, 178–184.
13 Carrasquer, G., Xiaoyan, W., Kissel, D., Rehm, W.S., Schwartz, M. and Dinno, M. (1989) Biochim. Biophys. Acta 73–78.
14 Clausen, C., Reinach, P.S. and Marcus, D.C. (1986) J. Membr. Biol. 91, 213–225.
15 Candia, O.A. (1972) Am. J. Physiol. 223, 1053–1057.
16 Nagel, W. and Reinach, P. (1980) J. Membr. Biol. 56, 73–79.
17 Cole, K.S. (1972) Membrane, Ions and Impulses, pp. 12–59, University of California Press, Berkeley, CA.
18 Widdicombe, J.H., Gashi, A.A., Basbaum, C.B. and Nathanson, I.T. (1986) Exp. Lung Res. 10, 57–69.
19 Pappenheimer, J.R. (1987) J. Membr. Biol. 100, 137–148.
20 Madara, J.L. and Pappenheimer, J.R. (1987) J. Membr. Biol. 100, 149–164.
21 Rick, R., Beck, F.X., Dorge, A. and Thurau, K. (1987) J. Membr. Biol. 95, 229–240.
22 Clausen, C., Machen, T.E. and Diamond, J. (1983) Biophys. J. 41, 167–177.